Astronomy & Astrophysics manuscript no.
(will be inserted by hand later)

arXiv:astro-ph/0209032v1 2 Sep 2002

A Substellar Mass Function for Alpha Per*

David Barrado y Navascués[1], Jerôme Bouvier[2], John R. Stauffer[3], Nicolas Lodieu[4], and Mark J. McCaughrean[4]

[1] Laboratorio de Astrofísica Espacial y Física Fundamental, INTA, P.O. Box 50727, E-28080 Madrid, Spain e-mail: `barrado@laeff.esa.es`
[2] Laboratoire d'Astrophysique, Observatoire de Grenoble, Université Joseph Fourier, B.P. 53, 38041 Grenoble Cedex 9, France e-mail: `jerome.bouvier@obs.ujf-grenoble.fr`
[3] IPAC, California Institute of Technology, Pasadena, CA 91125, USA e-mail: `stauffer@ipac.caltech.edu`
[4] Astrophysikalisches Institut Potsdam, An der Sternwarte 16, D-14482 Potsdam, Germany e-mail: `nlodieu@aip.de,mjm@aip.de`

Received ; accepted

Abstract. We present a deep, wide-field optical survey of the young stellar cluster Alpha Per, in which we have discovered a large population of candidate brown dwarfs. Subsequent infrared photometric follow-up shows that the majority of them are probable or possible members of the cluster, reaching to a minimum mass of 0.035 $M_\odot$. We have used this list of members to derive the luminosity and mass functions of the substellar population of the cluster (α=0.59±0.05, when expressed in the mass spectrum form $\phi \propto M^{-\alpha}$) and compared its slope to the value measure for the Pleiades. This comparison indicates that the two cluster mass functions are, indeed, very similar.

Key words. open clusters and associations: individual: Alpha Per – Stars: brown dwarfs – Stars: luminosity, mass functions

1. Introduction

In an ongoing effort to discover low-mass stars and brown dwarfs (BDs) belonging to young open clusters, we have studied the association Alpha Per. This is well-known nearby cluster with $(m-M)_0$=6.23 (176 pc). The interstellar reddening is also low, A_V=0.30 (Pinsonneault et al. 1998). The normally quoted age for the cluster, based on isochrone fitting of the upper main sequence (MS), is of order 50 Myr (cf. Meynet et al. 1993), though models with a larger amount of convective core overshoot can yield ages up to about 80 Myr (Ventura et al. 1998). Recently, using the data we published in a preliminary study of the BD population of the cluster (Stauffer et al. 1999), we estimated the age as 90 Myr, based on the location of the lithium depletion boundary. The theoretical background to this method can be found in Kumar (1963) and D'Antona and Mazzitelli (1994), and when applied to the Pleiades (Basri et al. 1996, Rebolo et al. 1996; Stauffer et al. 1998a) and IC 2391 (Barrado y Navascués et al. 1999) has also yielded ages ∼50% older than previously assumed. A review of these results may be found in Basri (2000).

During the last years, different clusters and star forming regions have been studied intensively and their BD population revealed. The Pleiades, Alpha Per cluster, IC2391, M35, NGC2516, Taurus, the Trapezium cluster, Sigma Orionis cluster, Cha I dark cloud, Upper-Sco OB association, and IC348 have been investigated (Rebolo et al. 1995; Festin 1997; Bouvier et al. 1998; Stauffer et al. 1998ab, 1999; Briceño et al. 1998; Barrado y Navascués et al. 1999, 2001ab, 2002; Neuhäuser & Comeron 1999; Zapatero-Osorio et al. 1999, 2000; Lucas & Roche 2000; Luhman 1999, 2000; Martín et al. 1999, 2000, 2001; Béjar et al. 2001; Pinfield et al. 2000; Ardila et al. 2000; Najita et al. 2000; Moraux et al. 2001; *et cetera*). All these works show that BDs are quite numerous and that the mass function (MF) usually presents an increase for very low-mass objects. In any case, the total mass below the substellar limit only contributes a few percent to the total mass of the parent cluster, at least in the case of the Pleiades (∼3-5 %, Bouvier et al. 1998, Hodgkin & Jameson 2000). However, it is not clear whether this MF is universal and this result can be extrapolated to other young clusters.

In this paper, we present a new deep, wide-field optical survey of the Alpha Per cluster. We have followed-up the optical candidates in the near-infrared using new infrared imaging data and the 2MASS catalogue (Skrutskie et al. 1997). Using this wealth of data, we have been able to

---

Send offprint requests to: D. Barrado y Navascués

* Based on observations collected with the Kitt Peak National Observatory, USA, and the Hispano-German Observatory of Calar Alto, Spain

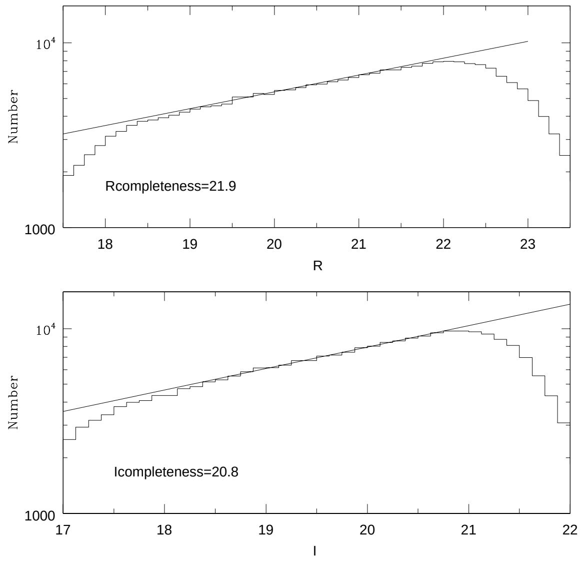

Fig. 1. Completeness of our KPNO/MOSA survey. For candidate members of the Alpha Per cluster, the survey is complete down to I_c=19.5, $(R\text{-}I)_c$=2.4

Table 1. Field centers for KPNO 4m CCD Mosaic Images

Field	R.A.	DEC
	(2000.0)	
A	03:27:10.0	49:24:00.0
B	03:28:00.0	48:42:00.0
C	03:24:50.0	48:42:00.0
D	03:21:40.0	48:42:00.0
E	03:19:35.0	49:27:00.0
F	03:33:45.0	49:35:00.0
G	03:33:45.0	49:04:00.0
H	03:33:45.0	48:34:00.0
I	03:33:45.0	50:06:00.0
J	03:30:30.0	50:09:00.0
K	03:27:00.0	50:13:00.0
L	03:23:10.0	48:11:00.0
M	03:21:00.0	50:48:00.0

establish the presence of a substantial population of BDs in the cluster, and derived its substellar MF.

2. Observations

2.1. Optical survey

We obtained deep optical imaging of the Alpha Per open cluster using the KPNO 4-m CCD mosaic camera, MOSA, on November 19–22 1998. Field centres were selected in order to cover as much of the central part of the cluster as possible while avoiding the brightest stars in the field (Table 1). All of the images were obtained with the facility R and I filters. Weather during the run was variable: Nov. 19 was generally overcast with periods of only moderate cirrus; Nov. 20 was clear but with extremely poor seeing; Nov. 21 was clear with good seeing; and Nov. 22 was again partly cloudy. In order to provide calibrated photometry for all stars, we overlapped the survey fields so as to provide photometric calibration even for fields whose deep images were obtained through light cirrus. The average seeing for the deep images was of order 1.0 arcseconds. For most fields, we obtained two 900 second R images and two 420 second I images; a few of the fields just designed to tie together the photometry were only observed with 100 or 200 second exposures. In all, we obtained deep imaging of 13 fields, thus corresponding to a total area on the sky of order 3 square degrees. Photometric calibration was derived from short exposures of three Landolt (1992) fields in SA92, SA98 and SA101. Initial results from analysis of the shorter exposures obtained during this run were reported by Stauffer et al. (1999).

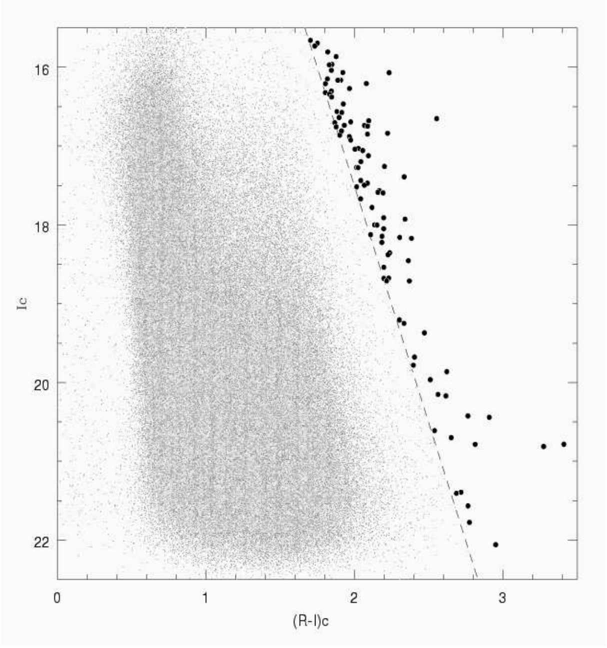

Fig. 2. Colour–Magnitude diagram in the fields we have studied. Solid circles represent the location of our initial selection of cluster candidates. The dashed line corresponds to the fiducial cluster main sequence.

2.2. Infrared follow-up

In addition to the KPNO/MOSA observations, we undertook several infrared observing campaigns at the Hispano-German Calar Alto Observatory in order to obtain additional data for candidate cluster members (see section 3.2). These runs included November 22–23 1999, using Omega-Cass (1024^2 pixels, 0.3 arcsec/pixel) on the 3.5-m telescope; February 16–21 2001 and November 6–7 2001, using MAGIC (256^2 pixels, 0.64 arcsec/pixel) on the 2.2-m telescope; and December 11–14 2000 and December 28–31 2001 using Omega-Prime (1024^2 pixels, 0.4 arcsec/pixel) on the 3.5-m telescope. We observed a total of 53 Alpha Per candidates in the magnitude range K'=13.0–19.2 magnitudes, equivalent to I_c=15.7–21.7 magnitudes.

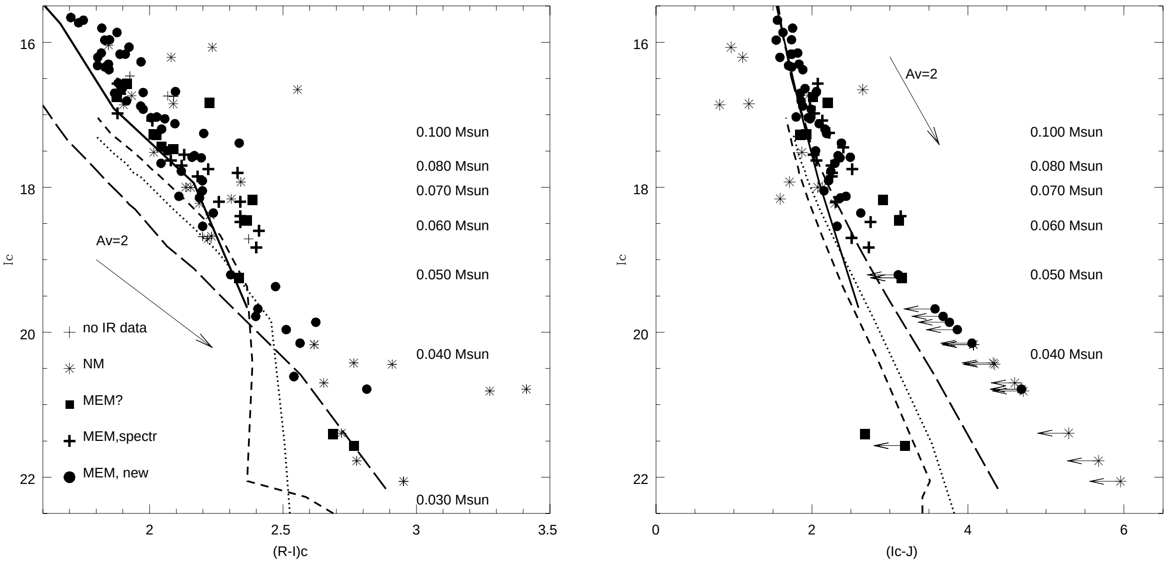

Fig. 3. Colour–Magnitude diagrams of Alpha Per cluster. See key for the meaning of the symbols. Three 80 Myr isochrones from Baraffe et al. (1998) and Chabrier et al. (2000) (NextGen model as long-dashed lines, Dusty model as dotted lines, and Cond model as short-dashed lines) are displayed together with a Leggett (1992) main sequence (solid lines). For several I_c magnitudes, the masses of cluster members are indicated in the right-hand side of each panel. We have included a reddening vector for A_V=2 for comparison purposes.

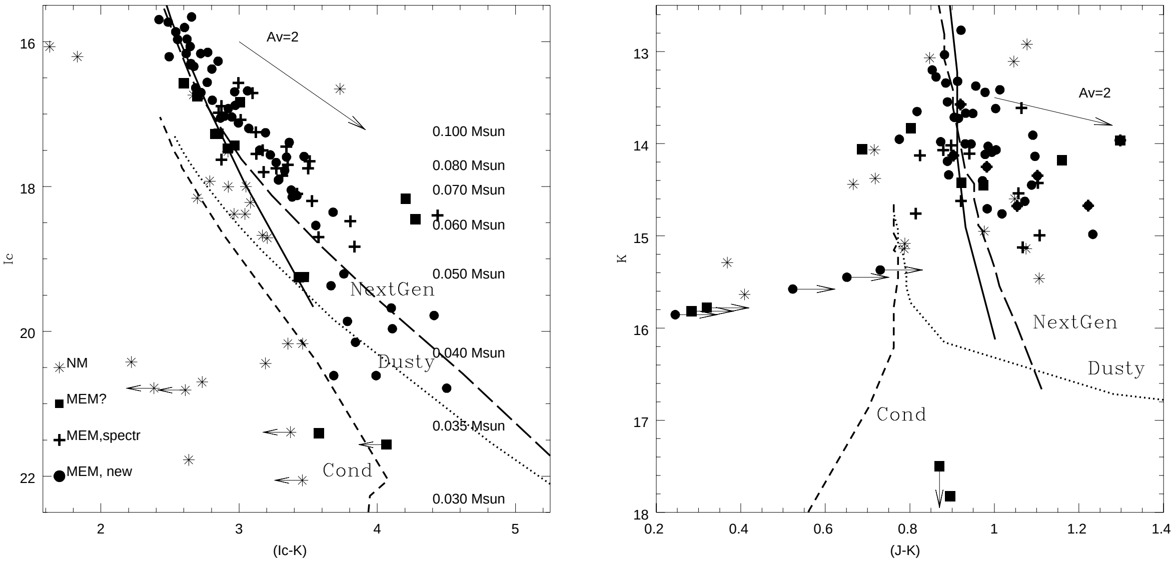

Fig. 3. (continue figure 3)

All were observed in the K' filter, while 24 were also measured at J, and a handful also at H.

We also searched the 2MASS point source catalogue (Skrutskie et al. 1997), in order to extend the infrared data coverage. Unfortunately, the present version of the 2MASS catalogue does not completely cover the Alpha Per cluster, due to gaps between the scans in that part of the sky. Moreover, the 2MASS survey does not go deep enough to detect all faint candidates in our survey. In summary, 47 of our candidates were found in the 2MASS catalogue; 25 additional candidates lie in the non-covered areas; and 21 are too faint to have been detected.

In total, all but two BD candidates derived from the optical KPNO MOSA data also have near-infrared photometry. Table 3 lists all available photometry.

2.3. Previously known Alpha Per members

In the following analysis of membership, we have also included previously-discovered photometrically-selected members of the cluster (Stauffer et al. 1999). Some of these also have low- and medium-resolution spectroscopy which supports their membership. We also searched the 2MASS catalogue for infrared photometry for these previously-known members (Table 2), for comparison with our MOSA-selected sample. Note, of course, that Alpha Per cluster contains other brighter and more massive members not analysed here (Stauffer et al. 1986, 1989; Prosser 1992, 1994, 1998).

3. Analysis

3.1. Optical photometry and coordinates

Raw photometry was derived using PSF–fitting, and calibrated using several standard stars (see section 2.1). We computed the initial coordinates by transforming the X,Y positions of each CCD to α, δ using field stars with known coordinates. The accuracy of this astrometry is better than 1 arcsec. Following this, we searched for the 2MASS counterparts, and when available, we used the much more accurate 2MASS astrometric positions in Table 3.

Our KPNO/MOSA optical data cover the range $16 \leq I_c \leq 22.5$, $0.0 \leq (R\text{-}I)_c \leq 3.5$. Figure 1 allows an estimation of the completeness limits. We have displayed two histograms with the number of detections in the R_c and I_c filters in a logarithmic form. The detections limits are located at the points where the histograms diverge from the straight lines (Wainscoat et al. 1992; Santiago et al. 1996). This is true for a region where field stars dominate the overall population, as in the case of the Alpha Per cluster (many more field stars than cluster members in a particular area). Therefore, for cluster members, we estimate that $I_{complete} \sim 20.75$ mag, $R_{complete} \sim 21.9$ mag. However, since the R_c filter effectively limits the completeness for cluster members, the actual values are $I_{complete} \sim 19.5$ mag, $(R-I)_{complete} \sim 2.4$. The detection limits reach $I_{limit} \sim 22.5$ mag, $R_{limit} \sim 25.5$ mag.

3.2. Optical colour-magnitude diagram

Figure 2 displays all the detections within our MOSA survey area. The straight dashed line denotes the position of a fiducial main sequence (i.e., the criterion we have used to select candidate members of the cluster). This line is an empirical zero age main sequence, shifted to fit the locus of previously known Alpha Per members. A total of 260,000 stars were detected, by far the majority of them field stars, fairly well separated from the cluster population by a fairly wide gap. This gap is not as sharp however as is seen in the Pleiades (Figure 2 of Bouvier et al. 1998), and thus we anticipate a stronger contamination of the cluster population in Alpha Per compared to the Pleiades: the latter cluster has a contamination of ∼30% (Bouvier et al. 1998; Martín et al. 2000; Moraux et al. 2001).

We have selected 94 candidate members based on the optical CMD. Since some of our fields overlap with each other, some of them have been detected twice, showing similar photometry. The candidate members are listed in Table 3. Figure 3a displays their location in an optical CMD. Bona fide members from Stauffer et al. (1999), based on optical-infrared data and spectroscopy are shown as thick crosses. Thin crosses denote the location of new candidates with no infrared data. Non-members, based on the new available data (see next section), appear as asterisks. Finally, possible and probable new members are shown as solid squares and circles, respectively. Also plotted are three 80 Myr isochrones from Baraffe et al. (1998) and Chabrier et al. (2000) (NextGen model as long-dashed line, Dusty model as dotted line, and Cond model as short-dashed line), along with a Leggett (1992) empirical main sequence for the cluster, plotted as a solid line. The I_c magnitudes of Alpha Per members with different masses, derived with a 80 Myr NextGen isochone, are also indicated.

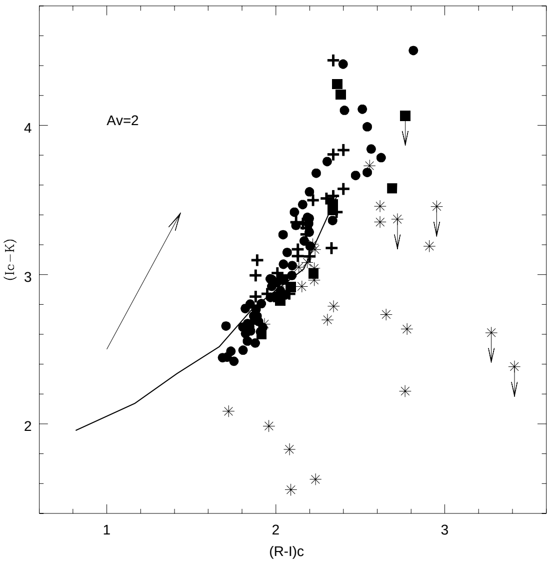

Fig. 4. Optical-IR Colour-Colour Diagram for Alpha Per cluster. Symbols as in Figure 3. The solid line comes from Leggett (1992).

Note that all colour-magnitude and colour-colour diagrams presented in this paper (this and next subsections) have made use of the following reddening values: $A_I=0.179$, $A_J=0.085$, $A_K=0.034$, and $E(V\text{-}I_c)=0.121$, $E(R\text{-}I)_c=0.067$, $E(I_c\text{-}J)=0.094$, $E(I_c\text{-}K)=0.145$, and $E(J\text{-}K)=0.051$. These values were derived from $A_V=0.30$, $R_V=3.12$ and the interstellar extinction law and transformation equation between filters and systems published by Rieke & Lebofsky (1985) and Taylor (1986).

3.3. Infrared data and membership selection

Alpha Per candidate members brighter than I=18.5 are expected to be detected by the 2MASS survey (Skrutskie et al. 1997), which reaches about $K \sim 15$. We have searched in this database and extracted the IR photometry for them. However, 2MASS has several patches in the Alpha Per area, with gaps between the images and some of our candidates were not observed. For objects at the faint end of 2MASS and fainter than it, we have carried out our own deep IR observations. All these data are listed in Table 3.

Figures 3b, c, and d show optical/IR-colour magnitude diagrams for the candidates derived from the KPNO, Calar Alto, and 2MASS data (Table 3). Symbols are as in Figure 3a (see key or section 3.2). As in the case of panel a, a reddening vector for A_V=2.0 has been included for comparison purposes. Note that neither of the two isochrones fully agree either with the new MOSA data or with the previously discovered bona fide members (Stauffer et al. 1999). This is perhaps not unexpected, as even these models which include state-of-the-art model atmospheres do not as yet accurately reproduce the optical SED's for late type stars and hence, in particular, the R band magnitudes are only approximate for the very cool objects in our figures. Figure 4 shows an optical-infrared colour-colour diagram for the same sample. The solid line corresponds to an empirical main sequence based on Leggett (1992) data. Objects with full agreement between their photometric locations in the four colour-magnitude diagrams and those expected for bona fide cluster members are henceforth classified as probable cluster members. Others, with slight disagreements in their photometry are classified as possible members. Finally, some (shown as asterisks) could be readily rejected as cluster members. The classification of each object is shown in the last column of Table 3. Out of the initial 94 candidates, more than half (54) have been classified as probably cluster members and 12 as possibles, while 26 objects turn out to be non-members. The remaining 2 candidates do not have infrared photometry and cannot be classified. Thus, the contamination of the sample lies in the range 30–45%, similar or larger than in the case of the Pleiades (Bouvier et al. 1998; Martín et al. 2000; Moraux et al. 2001).

3.4. Luminosity and Mass Functions

3.4.1. Luminosity Function

We have computed the cluster luminosity function (LF) at the end of the main sequence. We have done this both before and after rejecting the non-members from our initial membership list. The LF is illustrated in Figure 5, where we represent the histograms computed with the initial and final candidate members as solid circles (solid and dashed lines, respectively) and a control group of objects selected in the same fashion, but with colours bluer than them, with an arbitrary shift of $\Delta(R\text{-}I)$=–0.2 mag. Based on this selection criterion, the vast majority of the comparison sample should be field stars, at a distance similar to that of the cluster stars. The dotted segment represents the location of the completeness limit, which corresponds to ∼0.05 $M_\odot$. Poisson noise for each value is represented with the vertical error bar. Note that apparent I_c magnitudes are displayed at the bottom x-axis, whereas absolute magnitudes are represented at the top x-axis. The Alpha Per cluster LF presents two peaks (at this magnitude range): one at M(I_c)∼10 and another at 14.5 magnitudes. In the first case, the peak appears both in the Alpha Per member list and in the control group described above. In the second case, the sample is not complete, and it could be strongly influenced by pollution by spurious members, as the comparison with the control group suggests. Note that the peak at M(I_c)∼10 is present in some other young clusters, including the Pleiades (Zapatero Osorio 1997), but not all, for example, NGC 2516 (Jeffries et al. 2001; Barrado y Navascués et al. 2002), a rich, ∼125 Myr old cluster that is either slightly metal deficient (Jeffries et al. 1997, 1998, 2001) or approximately solar metallicity (Debernardi and North 2001; Terndrup et al. 2002). The peak in the LF for NGC2516 appears to occur about a magnitude fainter than for the Pleiades and Alpha Per (that is, at about M(I_c)∼11). Another similar age cluster, M35, appears to have the peak occur at about M(I_c)∼9 (Barrado y Navascues et al 2001a). Therefore, the exact absolute magnitude of the peak does not seem to be universal, at least for 100-200 Myr clusters.

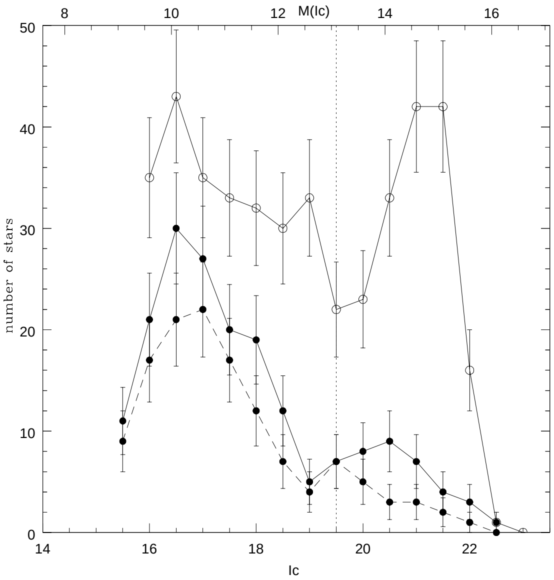

Fig. 5. Luminosity Function of Alpha Per cluster. The lower LFs correspond (solid circles) to the initial MOSA candidate members of the cluster, whereas the upper curve (open circles) was derived for a comparison sample of field stars. In the first case, we show the LF before and after rejecting the non-members (solid and dashed lines, respectively).

The gap in the Alpha Per LF at M(I_c)∼12.5 (corresponding to M6-M8 spectral type or about 0.055 $M_\odot$ for an age of 80 Myr) has been also found in other clusters. This is the case of the young cluster IC2391 (Barrado y Navascués et al. 2001b). Jameson (2002) noticed that this gap, which appears at about M7 spectral type, is present in clusters with ages ranging from few million years (Sigma

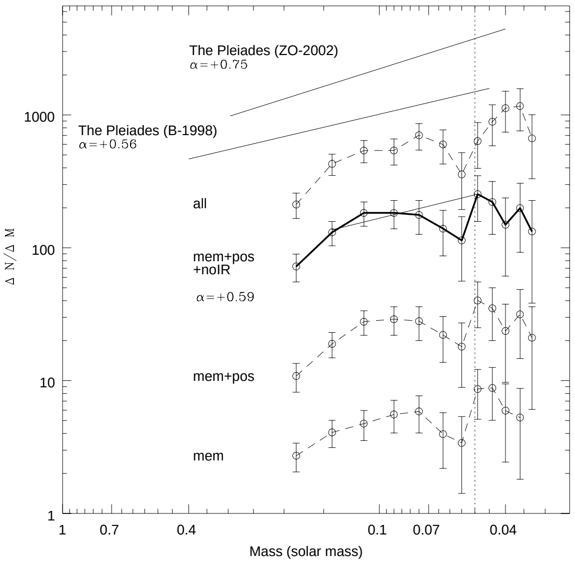

Fig. 6. Mass functions for the Alpha Persei cluster, illustrating the effect of contamination by field stars. These MFs were derived using a 80 Myr isochrone (Baraffe et al. 1998). The most probable MF is shown as a thick line. A linear fit for this MF is also included, with a power law index of α=0.59±0.05. For comparison, we have included the Pleiades MF by Bouvier et al. (1998), valid between 0.40 and 0.045 $M_\odot$ and by Zapatero Osorio el at. (2002), which was derived for the mass range 0.3–0.040 $M_\odot$.

Orionis cluster), up to at least seven hundred million year (Praesepe). It is clearly seen in the Pleiades too. They suggested that it could be related to the formation at these temperatures of large dust grains, although it might be related to some specific behavior in the luminosity–mass relationship or to the formation mechanism of these low mass objects (the efficiency of the fragmentation and collapse for cores with this mass range within the parental molecular cloud).

3.4.2. Mass Function

We have computed the Mass Function of the Alpha Per cluster using the non-dusty (Next-Gen) models by Baraffe et al. (1998) Note that the global behavior of the MF is not strongly affected by the particular set of isochrones, as we have shown in the case of M35 (Barrado y Navascués et al. 2001a) and NGC2516 (Barrado y Navascués et al. 2002), using evolutionary tracks from Baraffe et al. (1998), D'Antona & Mazzitelli (1994, 1997) and Siess et al. (2000). In order to assess the effects of contamination by field stars in our survey, and biases due to incomplete coverage in the infrared, we have estimated the MF based on several different subsamples of the candidate list. For the first sample, we used the full candidate list derived from the optical data only. In the second, we removed definite non-members. In the third, we removed sources without infrared photometry. Finally, in the fourth, we included only those sources classified as probable cluster members. All four derived MFs are shown in Figure 6 along with the MF for the Pleiades (Bouvier et al. 1998; Moraux et al. 2001; Zapatero Osorio et al. 2002).

Overall, the behaviour of the Alpha Per cluster MF is very similar to that of the Pleiades, both in the overlapping mass range and for less massive brown dwarfs. However, the MF of the Alpha Per cluster shows some possible structure, with a dip about 0.055 $M_\odot$ and a drop beyond 0.035 $M_\odot$, regardless the cluster age in the range 50–100 Myr (see next paragraph). Unfortunately, the uncertainties are large, the completeness limit of our MOSA survey is about 0.050 $M_\odot$, and there is significant pollution by field stars below this mass (peaking at about 0.030 $M_\odot$).

Figure 7 shows several realisations of the Alpha Per MF as a function of age (50, 80, and 100 Myr), using the complete list of candidates minus the definite non-members (Section 3.2). MFs have been derived for both the non-dusty Baraffe et al. (1998) and Burrows et al. (1997). Masses were derived either from the $M(I_c)$ magnitude (Baraffe et al. 1998 list these values) or from the bolometric luminosities (after Monet et al. 1992). It is readily seen that the slope, within the uncertainties, and the general shape of the cluster MF is essentially independent of the adopted age or the model. The exact mass of the dip in the MF (assuming it is real), however, does shift slightly depending on the age.

When defining the MF as $\phi \propto M^{-\alpha}$ (or more properly, the mass spectrum), the spectral index α indicates the slope in the diagram we show in Figure 6. We have fit a power law function to this MF, obtaining α=0.59±0.05. For the Pleiades, this index is 0.6, as derived by Bouvier et al. (1998). See also Martín et al. (2000); Hodgkin & Jameson (2000); Moraux et al. (2001); Zapatero Osorio et al. (2002) –α=0.75; and references therein. Two of the Pleiades MFs are shown in Figure 6. Béjar et al. (2001) have derived a MF for the younger cluster Sigma Orionis, about 5 Myr, down to the planetary mass domain at ∼0.013 $M_\odot$. This MF is shown in Figure 7. The spectral index of Sigma Orionis cluster (α=0.8±0.4) also agrees quite well, within the uncertainties, with both Alpha Per cluster and the Pleiades. Note that the Alpha Per data corresponding to the gap at 0.055 $M_\odot$ have not been included in this fit. In any case, independently of the power law index of the MF, Figures 6 and 7 clearly show that the MF keeps rising well below the substellar limit for Alpha Per cluster.

3.5. Brown dwarfs in the cluster

Recently, both Stauffer et al. (1999) and Basri & Martín (1999) searched for evidence of BDs in the Alpha Per cluster. Previously, Rebolo et al. (1992) and Zapatero Osorio et al. (1996) tried, without success, to find them in this association. Stauffer et al. (1999) included both low and

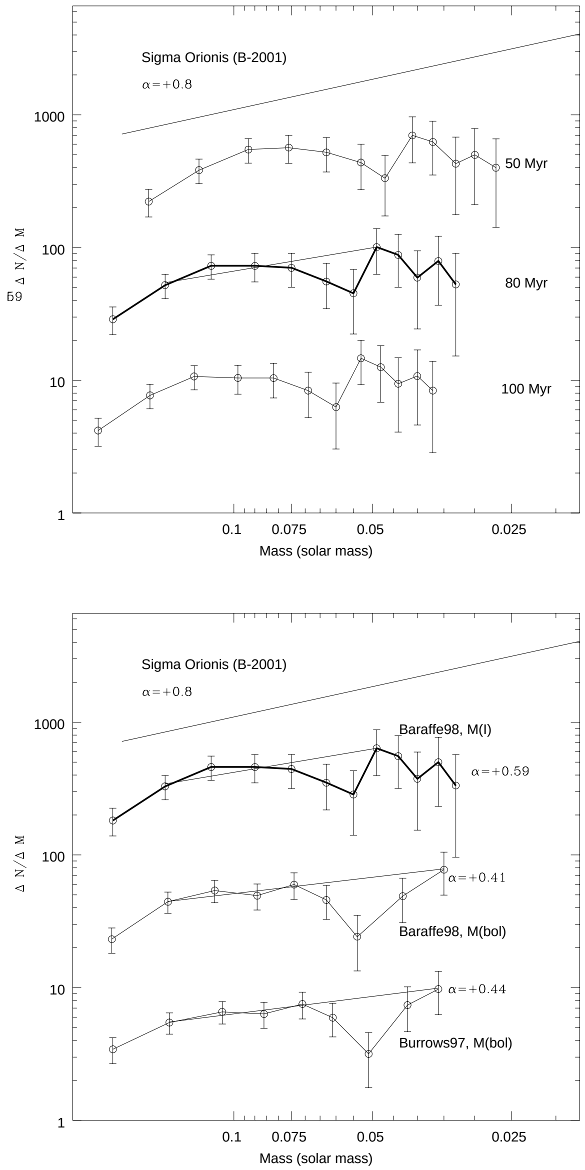

Fig. 7. Mass functions of Alpha Persei, illustrating the effect of the assumed age (panel a) and the choice of theoretical models (panel b). A power law fit and its slope is included in each case. A MF for the Sigma Orionis cluster (Béjar et al. 2001) is shown for comparison purposes (solid segment).

medium resolution spectroscopy, and some infrared photometry, establishing the location of the lithium depletion boundary (with the lithium age of the cluster, 90±10 Myr) and the member list of bona fide members (based on rough radial velocity, lithium detection, Hα emission, spectral types, *et cetera*). Since their spectroscopic data go down to I_c=18.7, and the stellar/substellar boundary is located at I_c=18.2 (Baraffe et al. 1998), they were able to catalogue 2 objects as probable brown dwarfs (another 3, which were catalogued as possible members, could also be BDs). In our new MOSA sample, there are 27 objects below the substellar frontier. Out of these 27 objects, 11 have infrared photometry which indicates that they are probable members of the cluster and, therefore, brown dwarfs. Another 5 have been classified as possible members and could be BDs if their membership is confirmed. The minimum mass is 0.035 M$_\odot$. Therefore, it seems likely that we have discovered a substantial population of BDs in the Alpha Per cluster. Note that it is difficult to use the proper motion method to establish Alpha Per membership, since its proper motion (22.93 mas/yr in α and –25.56 mas/yr in δ, Robichon et al. 1999), is large enough to be measured, but is also shared by a large fraction of the field stars (see, e.g., Prosser 1992). Therefore, only additional spectroscopic data (or better, a combination of optical and infrared photometry, proper motions and spectroscopy) will demonstrate beyond any reasonable doubt that the faint objects listed in our sample are, indeed, brown dwarfs.

4. Summary

Optical and near infrared photometry have been used to select a list of probable and possible low-mass members belonging to the young cluster Alpha Per, unveiling a large population of brown dwarf candidates. This information has been used to derive the luminosity and mass function of the cluster in the substellar domain. The index of the mass function, α = 0.59, is very similar to that determined for the Pleiades (120 Myr) and σ Orionis (2–8 Myr) clusters.

Acknowledgements. DBN and JRS acknowledge the hospitality of the Observatoire de Grenoble during the preparation of this paper. We thank D. Montes for his help collecting part of the IR data and M.R. Zapatero Osorio for her comments on an early version of this paper. JB, NL, and MJM acknowledge support from the EC Research Training Network "The Formation and Evolution of Young Stellar Clusters" (HPRN-CT-2000-00155). This work has been partially financed by Spanish *"Programa Ramón y Cajal"* and AYA2001-1124-CO2 programs.

References

Ardila D.R., Martín E.L., Basri G., 2000, AJ 120, 479
Baraffe I., Chabrier G., Allard F., Hauschildt P. H., 1998, A&A, 337, 403
Barrado y Navascués D., Stauffer J.R., Patten, B.M., 1999, ApJ Letters 522, L56
Barrado y Navascués D., Stauffer J.R., Bouvier J., Martín E.L., 2001, ApJ 546, 1006
Barrado y Navascués D., Stauffer. J.R., Briceño, C., Patten B., Hambly N.C., Adams, J.D., 2001, ApJ Suppl. 134, 103
Barrado y Navascués D., Stauffer. J.R., et al. 2002, in prep.
Basri G., Martín E.L., 1999, 510, 266
Basri G., Marcy G.W., Graham J.R., 1996, ApJ 458, 600
Basri G., 2000, Ann. Rev. A&A 38, 485
Béjar V., Martín E.L., Zapatero Osorio M.R., Rebolo R., Barrado y Navascués D., Bailer-Jones C.A.L., Mundt R., Baraffe I., Chabrier C., Allard F., 2001, ApJ 556, 830
Bouvier J., Stauffer J.R., Martín, E.L., Barrado y Navascués, D., Wallace B., Béjar, V., 1998, A&A 336, 490

Table 2. Previusly known Alpha Per members from Stauffer et al. (1999). Data from 2MASS survey.

Name	J	H	Ks
AP300	15.595 0.061	14.859 0.074	14.538 0.083
AP301	15.233 0.061	14.526 0.072	14.251 0.082
AP302	15.572 0.066	15.101 0.092	14.758 0.102
AP303	14.951 0.043	14.278 0.049	14.127 0.062
AP304	16.102 0.107	15.418 0.134	14.995 0.130
AP305	15.729 0.077	14.906 0.084	14.675 0.100
AP306	16.240 0.111	15.727 0.160	15.077 null
AP306	15.262 0.050	14.522 0.063	13.964 0.051
AP307	14.948 0.043	14.280 0.055	14.069 0.060
AP308	14.677 0.035	14.128 0.048	13.613 0.049
AP309	14.495 0.032	13.882 0.044	13.575 0.045
AP275	15.031 0.046	14.488 0.059	14.128 0.066
AP310	15.543 0.065	15.110 0.104	14.622 0.085
AP311	15.450 0.058	14.709 0.069	14.348 0.069
AP312	16.274 0.118	15.483 0.131	15.132 0.135
AP313	15.528 0.066	15.035 0.103	14.425 0.081
AP314	16.196 0.107	15.433 0.128	15.133 0.151
AP315	15.894 0.089	15.234 0.111	14.672 0.104
AP318	15.049 0.049	14.502 0.068	14.108 0.071
AP319	14.916 0.053	14.378 0.063	14.018 0.069
AP326	16.192 0.108	15.556 0.125	15.125 0.149

Briceño C, Hartmann L., Stauffer J.R., Martín E.L., 1998, AJ 115, 2074

Burrow et al. 1997, ApJ 491, 856

Chabrier G., Baraffe I., Allard F., Hauschildt P., 2000, ApJ, 542, L119.

D'Antona F., & Mazzitelli I. 1994 ApJ Suppl. 90, 467

D'Antona F., & Mazzitelli I. 1997, in "Cool Stars in Clusters and Associations", ed. R. Pallavicini & G. Micela, Mem. Soc. Astron. Italiana, 68 (4), 807

Festin L., 1997, A&A 322, 455

Hodgkin S.T., Jameson R.F., 2000, in "Stellar Clusters and Associations: Convection, Rotation, and Dynamos". R. Pallavicini, G. Micela and S. Sciortino (eds.) ASP Conf. Series 198, 245

Jeffries R.D., Thurston M.R., Pye J.P., 1997, MNRAS 287, 350

Jeffries R.D., James D., J., Thurston M.R., 1998, MNRAS 300, 550

Jeffries R.D., Thurston M.R., Hambly N.C., 2001, A&A 375, 863

Jameson R.F., 2002, in "Brown Dwarfs", IAU Symposium 211, eds. E.L. Martín, in press

Koester D., Reimers D., 1996, A&A 313, 810

Kumar S.S., 1963, ApJ 137, 1121

Landolt A., 1992, AJ 104, 340

Leggett S., 1992 ApJ SS 82, 351

Lucas P.W:, Roche P.F:, 2000, MNRAS 314, 858

Luhman K.L., 1999, ApJ 525, 466

Luhman K.L., 2000, ApJ 544, 1044

Martín E.L., Brandner W., Bouvier J., Luhman K.L., Stauffer, J., Basri G., Zapatero Osorio M.R., Barrado y Navascués D., 2000, ApJ 543, 299

Martín E.L., Zapatero Osorio M.R., Barrado y Navascués D., Béjar V., Rebolo R., 2001, ApJ 558, 117

Meynet G., Mermilliod J.-C., Maeder A., 1993, A&A Series 98, 477

Monet D., et al. 1992, AJ 103, 638.

Moraux E., Bouvier J, Stauffer J., 2001, A&A 367, 211

Najita J.R., Tiede G.P., Carr J.S., 2000, ApJ 541, 977

Neuhäuser R., Comeron F., 1999, A&A 350, 612

Pinfiled D.J., Hodgkin S.T., Jameson R.F., Cossburn M.R., Hambly N.C., Devereux N., 2000, MNRAS 313, 347

Pinsonneault M.H., Stauffer J., Soderblom D,R., King J.R., Hanson R.B., 1998, ApJ 504, 170

Prosser C.F., 1992, AJ 103, 488

Prosser C.F., 1994, AJ 107, 1422

Prosser C.F., Randich S., Stauffer J.R., Schmitt J. H. M. M., Simon T., 1996, AJ 112, 1570

Prosser C.F., 1998, Astron. Nachr. 319, 215

Rebolo R., Martín E.L., Magazzù A., 1992, ApJ Letters 389, 83

Rebolo R., Martín E.L., Basri G., Marcy G.W., Zapatero-Osorio M.R., 1996, ApJ 469, 706

Rebolo R, Zapatero Osorio M.R., Martín E.L., 1995, Nature 377, 129

Rieke G.H. & Lebofsky M.J., 1985, ApJ 288, 618

Robichon N., Arenou F., Mermilliod J.-C., Turon C., 1999, A&A 345, 471

Santiago B.X., Gilmore G., Elson R.A.W., 1996, MNRAS 281, 871

Siess L., Dufour E., Forestini M., 2000, A&A 358, 593

Skrutskie M. F., Schneider S. E., Stiening R., Strom S. E., Weinberg M. D., Beichman C., Chester T., Cutri R., Lonsdale C., Elias J., Elston R., Capps R., Carpenter J., Huchra J., Liebert J., Monet D., Price S., Seitzer P. in "The Impact of Large Scale Near-IR Sky Surveys", eds. F. Garzon et al., p. 25. Dordrecht: Kluwer Academic Publishing Company, 1997

Stauffer J. R., Hartmann L. W., Burnham J. N., Jones B. F. 1985 ApJ 289 247

Stauffer John R., Hartmann Lee W., Jones Burton F. 1989 ApJ 346 160

Stauffer J.R., Schultz G., Kirkpatrick J.D., 1998, ApJ Letters 499, 199

Stauffer J.R., Barrado y Navascués D., Bouvier J., et al. 1999, ApJ 527, 219

Taylor B.J., 1986, ApJ Suppl.Series 60, 577

Ventura P., Zeppieri A., Mazzitelli I., D'Antona F., 1998, A&A 334, 953

Wainscoat R.J., Cohen M., Volk K., Walker H.J., Schwartz D.E., 1992, ApJ Suppl., 83, 111

Zapatero Osorio M.R., Rebolo R., Martín E.L., García López R., 1996, A&A 305, 519

Zapatero Osorio M.R., 1997, PhD. Universidad de La Laguna, Spain

Zapatero Osorio M.R., Rebolo R., Martín E.L., Hodgkin S.T., Cossburn M.R., Magazzù A., Stelle I.A., Jameson R.F., 1999, A&A Suppl. 134, 537

Zapatero Osorio M.R., Béjar V.J.S., Martín E.L., Rebolo R., Barrado y Navascués D., Bailer-Jones C.A.L., Mundt, R., 2000, Science 290, 103

Zapatero Osorio M.R., et al. 2002, private communication.

Table 3. α Per data from KPNO/MOSA 1998. Probable members, possible members, probable non-members, and no IR data.

ID	alpha delta (J2000.0)	I_c	$(R-I)_c$	δI δR	J	H	Ks	J	K'	Source	Mem.
					2MASS						
AP282	3 24 22.55 +48 24 26.1	15.217	1.712	0.020 0.002	13.690 0.030	13.019 0.035	12.769 0.033	– –	– –	–	Y
AP283	3 24 38.78 +48 17 17.1	15.696	1.752	0.015 0.003	14.138 0.030	13.520 0.036	13.276 0.044	– –	– –	–	Y
AP301	3 18 09.05 +49 25 19.0	17.594	2.194	0.004 0.005	15.233 0.062	14.526 0.072	14.251 0.082	14.970 0.019	13.854 0.021	b	Y
AP305	3 19 21.60 +49 23 31.0	18.355	2.239	0.009 0.012	15.729 0.078	14.906 0.084	14.675 0.100	15.774 0.014	14.703 0.018	b	Y
AP306	3 19 41.32 +50 30 45.1	18.171	2.385	0.003 0.008	15.262 0.051	14.522 0.063	13.964 0.051	– –	– –	–	Y?
AP309	3 22 40.65 +48 00 33.6	16.378	1.848	0.003 0.002	14.495 0.035	13.882 0.045	13.575 0.046	– –	– –	–	Y
AP311	3 23 08.67 +48 04 50.6	17.497	2.067	0.004 0.005	15.450 0.060	14.709 0.070	14.348 0.070	– –	– –	–	Y
AP315	3 26 34.10 +49 07 46.1	18.049	2.198	0.009 0.012	15.894 0.090	15.234 0.111	14.672 0.104	15.899 0.022	14.982 0.032	b	Y
AP327	3 20 31.74 +49 39 59.6	15.056	1.959	0.089 0.016	13.917 0.035	13.388 0.038	13.070 0.037	– –	– –	–	N
AP328	3 21 25.61 +48 10 01.0	15.193	1.720	0.083 0.015	14.154 0.033	13.397 0.037	13.108 0.038	– –	– –	–	N
AP329	3 23 56.34 +48 09 21.0	15.479	1.685	0.026 0.002	13.917 0.030	13.290 0.033	13.035 0.035	– –	– –	–	Y
AP330	3 34 15.6 +49 58 48	15.659	1.705	0.006 0.027	– –	– –	– –	– –	13.003 0.008	d	Y
AP331	3 32 05.9 +50 05 55	15.731	1.734	0.033 0.042	– –	– –	– –	– –	13.244 0.009	d	Y
AP332	3 25 16.90 +48 36 09.0	15.805	1.821	0.003 0.010	14.053 0.036	13.410 0.040	13.200 0.035	– –	– –	–	Y
AP333	3 25 13.55 +50 27 33.0	15.865	1.878	0.014 0.008	14.236 0.031	13.603 0.034	13.323 0.039	– –	– –	–	Y
AP334	3 22 45.47 +48 21 33.1	15.965	1.850	0.013 0.004	14.227 0.034	13.641 0.041	13.342 0.036	– –	– –	–	Y
AP335	3 28 52.96 +50 19 25.9	15.970	1.832	0.034 0.008	14.428 0.041	13.761 0.040	13.415 0.047	– –	– –	–	Y
AP336	3 31 55.3 +49 08 31	16.039	1.846	0.026 0.214	– –	– –	– –	– –	14.659 0.031	d	N
AP337	3 34 07.5 +48 32 08	16.067	1.923	0.040 0.004	– –	– –	– –	– –	13.421 0.010	d	Y
AP338	3 24 52.65 +48 46 12.8	16.069	2.235	0.042 0.104	15.106 0.048	14.481 0.060	14.440 0.082	– –	– –	–	N
AP339	3 26 33.24 +50 07 41.7	16.148	1.819	0.043 0.003	14.331 0.037	13.734 0.037	13.375 0.037	– –	– –	–	Y
AP340	3 21 34.85 +48 16 28.7	16.164	1.909	0.002 0.002	14.436 0.034	13.781 0.041	13.547 0.043	– –	– –	–	Y
AP341	3 31 03.39 +50 24 41.6	16.165	1.889	0.008 0.002	14.421 0.040	13.794 0.046	13.443 0.047	– –	– –	–	Y
AP342	3 25 39.24 +48 45 21.1	16.207	2.081	0.011 0.068	15.095 0.044	14.447 0.057	14.377 0.075	– –	– –	–	N
AP343	3 23 48.48 +48 36 43.0	16.208	1.806	0.007 0.012	14.619 0.045	14.003 0.050	13.714 0.052	– –	– –	–	Y
AP344	3 26 52.0 +50 00 33	16.270	1.968	0.022 0.002	– –	– –	– –	– –	13.422 0.006	c	Y
AP345	3 33 45.8 +50 08 53	16.302	1.846	0.005 0.008	– –	– –	– –	14.468 0.010	13.651 0.012	d	Y
AP346	3 21 30.06 +48 49 23.2	16.321	1.805	0.050 0.022	14.621 0.037	13.979 0.045	13.672 0.047	– –	– –	–	Y
AP347	3 31 33.77 +49 52 02.1	16.342	1.833	0.007 0.004	14.601 0.045	13.967 0.050	13.669 0.055	– –	– –	–	Y
AP348	3 26 48.2 +48 44 00	16.466	1.926	0.032 0.009	– –	– –	– –	– –	– –	–	–
AP349	3 26 47.9 +50 02 16	16.562	1.883	0.011 0.002	– –	– –	– –	– –	13.793 0.005	c	Y
AP350	3 32 06.8 +49 25 23	16.574	1.916	0.024 0.009	– –	– –	– –	– –	13.974 0.020	d	Y?
AP351	3 28 47.8 +50 02 01	16.638	1.898	0.008 0.004	– –	– –	– –	14.727 0.033	13.952 0.019	d	Y
AP352	3 19 51.98 +48 48 22.6	16.652	2.555	0.009 0.007	13.999 0.030	13.344 0.035	12.922 0.037	– –	– –	–	N
AP353	3 24 48.66 +48 49 47.0	16.680	2.097	0.004 0.005	14.622 0.037	13.975 0.049	13.619 0.051	– –	– –	–	Y
AP354	3 27 31.64 +48 53 23.3	16.693	1.976	0.009 0.024	14.640 0.043	14.104 0.052	13.725 0.056	– –	– –	–	Y
AP355	3 22 33.15 +48 47 00.3	16.703	1.869	0.009 0.005	14.852 0.043	14.255 0.059	13.979 0.058	– –	– –	–	Y
AP356	3 18 22.06 +49 20 19.4	16.737	1.933	0.009 0.004	14.784 0.047	14.240 0.064	14.068 0.064	– –	– –	–	N
AP357	3 32 42.5 +49 50 10	16.740	2.068	0.015 0.004	– –	– –	– –	– –	– –	–	–
AP357	“ “	16.748	2.090	0.002 0.004	– –	– –	– –	– –	– –	–	–
AP358	3 34 37.8 +49 13 53	16.756	1.878	0.003 0.005	– –	– –	– –	14.745 0.011	14.058 0.021	d	Y?
AP359	3 23 37.13 +48 37 15.3	16.809	1.914	0.002 0.004	14.948 0.045	14.296 0.057	14.003 0.057	– –	– –	–	Y
AP360	3 32 24.0 +50 16 58	16.838	2.224	0.002 0.013	– –	– –	– –	14.634 0.010	13.831 0.016	d	Y?
AP361	3 23 14.03 +48 42 21.3	16.849	2.089	0.020 0.327	15.658 0.067	15.272 0.106	15.290 0.175	– –	– –	–	N
AP362	3 25 24.45 +48 45 21.3	16.862	1.902	0.008 0.070	16.045 0.087	15.800 0.161	15.636 0.225	– –	– –	–	N
AP363	3 24 00.33 +47 55 29.7	16.880	1.967	0.002 0.002	14.999 0.046	14.295 0.051	13.908 0.058	– –	– –	–	Y
AP364	3 20 39.16 +49 32 06.0	16.924	1.976	0.007 0.004	14.933 0.052	14.428 0.074	14.002 0.059	– –	– –	–	Y
AP365	3 28 22.94 +49 11 24.0	17.030	2.027	0.010 0.007	15.233 0.057	14.473 0.061	14.137 0.075	– –	– –	–	Y
AP366	3 26 35.50 +49 15 43.8	17.040	2.005	0.053 0.011	15.087 0.048	14.486 0.058	14.093 0.061	– –	– –	–	Y
AP367	3 34 40.80 +50 03 43	17.056	2.057	0.002 0.004	– –	– –	– –	15.080 0.015	14.191 0.017	d	Y
AP368	3 23 03.38 +48 53 05.8	17.123	2.095	0.004 0.007	15.031 0.048	14.488 0.060	14.128 0.067	– –	– –	–	Y
AP368	“ “	17.198	2.045	0.010 0.011	“ “	“ “	“ “	– –	– –	–	Y
AP369	3 26 44.9 +50 25 09	17.258	2.203	0.005 0.008	– –	– –	– –	15.071 0.011	14.067 0.012	d	Y
AP370	3 24 21.28 +48 58 59.5	17.271	2.015	0.003 0.007	15.342 0.056	14.724 0.080	14.420 0.081	– –	– –	–	Y?
AP371	3 23 59.92 +48 54 10.7	17.274	2.026	0.002 0.009	15.422 0.063	14.724 0.077	14.448 0.086	– –	– –	–	Y?
AP372	3 28 02.20 +48 41 07.2	17.391	2.336	0.010 0.010	15.013 0.050	14.465 0.054	14.028 0.058	– –	– –	–	Y
AP373	3 33 20.6 +48 45 49	17.437	2.044	0.007 0.016	– –	– –	– –	– –	14.469 0.021	d	Y?
AP374	3 32 18.8 +49 32 18	17.472	2.089	0.004 0.006	– –	– –	– –	– –	14.554 0.022	d	Y?
AP375	3 20 43.49 +50 59 39.6	17.518	2.016	0.007 0.014	15.647 0.069	15.223 0.121	14.599 0.095	15.225 0.025	14.263 0.031	b	N
AP376	3 32 43.7 +50 18 25	17.564	2.168	0.005 0.015	– –	– –	– –	15.230 0.019	14.338 0.029	b	Y
AP377	3 27 31.29 +48 39 23.3	17.586	2.159	0.015 0.019	15.094 0.055	14.482 0.071	14.116 0.071	14.896 0.007	13.905 0.018	b	Y
AP378	3 27 00.3 +49 14 38	17.670	2.043	0.010 0.010	– –	– –	– –	15.374 0.025	14.402 0.032	b	Y
AP379	3 29 18.74 +50 22 10.9	17.779	2.119	0.005 0.009	15.537 0.071	15.085 0.088	14.449 0.079	15.456 0.025	14.672 0.040	b	Y

a.- 1999 November. b 2000 February. c 2000 December. d 2001 November. e 2001 December

H data from CAHA: AP345 H=13.920±0.008, AP351 H=14.203±0.043, AP358 H=14.205±0.014, AP360 H=14.084±0.011, AP367 H=14.448±0.013, AP369 H=14.324±0.010

Table 3. (Continue) α Per data from KPNO/MOSA 1998. Probable members, possible members, probable non-members, and no IR data.

ID	alpha delta (J2000.0)	I_c	$(R-I)_c$	δI δR	J	H	Ks	J	K’	Source	Mem.
					2MASS						
AP380	3 25 03.79 +48 49 58.6	17.910	2.198	0.004 0.008	15.697 0.072	15.078 0.100	14.625 0.102	15.374 0.025	14.355 0.030	b	Y
AP381	3 28 06.3 +48 45 13	17.927	2.342	0.009 0.013	>16.1 –	>15.6 –	>15.3 –	16.214 0.045	15.139 0.062	b	N
AP382	3 33 48.08 +48 52 28	18.000	2.136	0.005 0.008	– –	– –	– –	15.926 0.029	14.950 0.030	b	N
AP383	3 32 22.8 +48 54 11	18.003	2.154	0.003 0.005	– –	– –	– –	15.870 0.023	15.082 0.039	b	N
AP384	3 27 40.03 +48 33 55.8	18.125	2.110	0.021 0.031	15.689 0.081	15.159 0.118	14.706 0.102	15.793 0.026	14.820 0.028	b	Y
AP385	3 20 07.42 +50 39 53.3	18.145	2.187	0.004 0.007	15.779 0.085	15.128 0.108	14.761 0.114	15.954 0.025	15.003 0.031	b	Y
AP386	3 22 02.3 +47 58 38	18.160	2.306	0.003 0.008	>16.1 –	>15.6 –	>15.3 –	16.568 0.046	15.462 0.053	b	N
AP387	3 18 19.32 +49 14 35.1	18.222	2.186	0.004 0.007	15.927 0.106	15.293 0.129	15.140 0.162	15.955 0.022	15.015 0.031	b	N
AP388	3 31 47.4 +50 03 25	18.380	2.227	0.005 0.008	– –	– –	– –	– –	15.337 0.040	d	N
AP388	“ “	“	“	“ “	– –	– –	– –	– –	15.416 0.084	e	N
AP389	3 27 41.21 +48 40 33.9	18.455	2.364	0.019 0.022	15.339 0.067	14.647 0.073	14.179 0.074	– –	– –	–	Y?
AP390	3 21 54.45 +48 33 14.9	18.538	2.199	0.006 0.009	16.216 0.295	15.531 0.151	14.983 0.172	– –	– –	–	Y
AP391	3 32 48.1 +49 52 26	18.675	2.232	0.012 0.014	– –	– –	– –	– –	15.506 0.050	d	N
AP391	“ “	18.710	2.218	0.005 0.008	– –	– –	– –	– –	“ “	“	N
AP392	3 28 27.1 +50 20 02	19.207	2.304	0.006 0.014	>16.1 –	>15.6 –	>15.3 –	– –	15.449 0.017	a	Y
AP393	3 29 08.2 +48 25 35	19.250	2.335	0.022 0.035	>16.1 –	>15.6 –	>15.3 –	– –	15.780 0.021	e	Y?
AP393	“ “	“	“	“ “	“ –	“ –	“ –	– –	15.816 0.080	d	Y?
AP394	3 35 26.0 +49 46 55	19.370	2.472	0.008 0.017	– –	– –	– –	– –	15.705 0.023	a	Y
AP395	3 24 44.5 +48 21 29	19.678	2.406	0.024 0.036	>16.1 –	>15.6 –	>15.3 –	– –	15.577 0.023	a	Y
AP396	3 28 16.0 +48 37 40	19.781	2.398	0.016 0.048	>16.1 –	>15.6 –	>15.3 –	– –	15.370 0.015	a	Y
AP397	3 21 21.8 +48 02 23	19.862	2.623	0.012 0.038	>16.1 –	>15.6 –	>15.3 –	– –	16.078 0.029	a	Y
AP398	3 22 38.0 +48 58 03	19.964	2.512	0.011 0.028	>16.1 –	>15.6 –	>15.3 –	– –	15.855 0.023	a	Y
AP399	3 25 48.5 +50 00 59	20.151	2.564	0.014 0.045	>16.1 –	>15.6 –	>15.3 –	– –	16.309 0.047	a	Y
AP400	3 28 48.0 +50 20 42	20.170	2.617	0.019 0.085	>16.1 –	>15.6 –	>15.3 –	– –	16.711 0.175	d	N
AP400	“ “	“	“	“ “	“ –	“ –	“ –	– –	16.817 0.090	e	N
AP401	3 23 43.5 +48 22 39	20.424	2.765	0.020 0.292	>16.1 –	>15.6 –	>15.3 –	– –	18.204 0.140	a	N
AP402	3 30 38.7 +50 16 39	20.442	2.909	0.020 0.257	>16.1 –	>15.6 –	>15.3 –	– –	17.251 0.064	e	N
AP403	“ “	“	“	“ “	– –	– –	– –	– –	16.926 0.185	d	Y
AP403	3 32 04.6 +49 20 48	20.611	2.541	0.020 0.053	– –	– –	– –	– –	16.62 0.08	e	Y
AP404	3 23 48.3 +48 29 03	20.700	2.653	0.030 0.125	>16.1 –	>15.6 –	>15.3 –	– –	17.967 0.112	a	N
AP405	3 29 13.0 +50 05 24	20.784	3.412	0.064 0.224	>16.1 –	>15.6 –	>15.3 –	– –	>18.4 –	e	N
AP406	3 23 09.9 +48 16 30	20.785	2.814	0.025 0.127	>16.1 –	>15.6 –	>15.3 –	– –	16.283 0.028	a	Y
AP407	3 23 59.3 +48 28 30	20.811	3.275	0.038 0.258	>16.1 –	>15.6 –	>15.3 –	– –	>18.20 –	e	N
AP408	3 26 36.0 +49 36 58	21.392	2.719	0.043 0.258	>16.1 –	>15.6 –	>15.3 –	– –	>18.02 –	e	N
AP409	3 20 17.7 +50 46 03	21.406	2.688	0.045 0.153	>16.1 –	>15.3 –	>15.3 –	18.723 0.266	17.827 0.164	a	Y?
AP410	3 26 21.6 +48 44 50	21.565	2.766	0.060 0.519	>16.1 –	>15.6 –	>15.3 –	>18.37 –	>17.5 –	a	Y?
AP411	3 26 10.1 +49 37 53	21.774	2.776	0.045 0.239	>16.1 –	>15.6 –	>15.3 –	– –	19.138 0.451	e	N
AP412	3 26 03.1 +49 30 29	22.057	2.952	0.071 0.342	>16.1 –	>15.6 –	>15.3 –	– –	>18.60 –	e	N

a.- 1999 November. b 2000 February. c 2000 December. d 2001 November. e 2001 December
H data from CAHA.